Microscopic structure of the Gamow-Teller resonance in ^{58}Cu

K. Hara,[1] T. Adachi,[2] H. Akimune,[3] I. Daito,[4] H. Fujimura,[1] Y. Fujita,[2] M. Fujiwara,[1,5] K. Fushimi,[6] K. Y. Hara,[3] M. N. Harakeh,[7] K. Ichihara,[6] T. Ishikawa,[8] J. Jänecke,[9] J. Kamiya,[1] T. Kawabata,[10] K. Kawase,[1] K. Nakanishi,[1] Y. Sakemi,[1] Y. Shimbara,[2] Y. Shimizu,[1] M. Uchida,[8] H. P. Yoshida,[1] M. Yosoi,[8] and R. G. T. Zegers[1]

[1]*Research Center for Nuclear Physics, Osaka University, Mihogaoka 10-1 Ibaraki, Osaka 567-0047, Japan*

[2]*Department of Physics, Osaka University, Toyonaka, Osaka 560-0043, Japan*

[3]*Department of Physics, Konan University, Kobe, Hyogo 658-8501, Japan*

[4]*Department of Physics, Nagoya University, Furo-Cho, Chikusa-Ku, Nagoya 464-8602, Japan*

[5]*Advanced Science Research Center, JAERI, Tokai, Ibaraki, 319-1195, Japan*

[6]*Department of Physics, University of Tokushima, Tokushima 770-8502, Japan*

[7]*Kernfysisch Versneller Instituut, 9747 AA Groningen, The Netherlands*

[8]*Department of Physics, Kyoto University, Kyoto 606-8502, Japan*

[9]*Department of Physics, University of Michigan, Ann Arbor, Michigan 48109-1120, USA*

[10]*Center for Nuclear Study, Graduate School of Science, University of Tokyo, Bunkyo, Tokyo 113-0033, Japan*

(Received 8 February 2003; revised manuscript received 6 October 2003; published 23 December 2003)

The Gamow-Teller (GT) states in ^{58}Cu have been studied via the ^{58}Ni(^{3}He, $t+p$) and ^{58}Ni(^{3}He, $t+\gamma$) coincidence experiments. The GT states in ^{58}Cu at E_x=6–12 MeV, where both T=1 and T=2, 1^+ states exist, are excited strongly in the ^{58}Ni(^{3}He, t) reaction at $E(^3\mathrm{He})$=450 MeV and θ=0°. Proton emissions from the GT states in ^{58}Cu to the hole states in ^{57}Ni have been observed with solid-state detectors in coincidence with high energy tritons measured with a magnetic spectrometer. For the first time, the γ-ray emissions from the excited states in ^{58}Cu and in ^{57}Ni, following the ^{58}Ni(^{3}He, $t+p$) reaction at intermediate energies, have also been observed in coincidence with tritons. Strengths of proton decay into several neutron-hole states in ^{57}Ni and γ-decay strengths are used to discuss the wave functions of the GT states in ^{58}Cu. The T=1 and T=2 GT states do only weakly decay into a T=3/2, $f_{7/2}^{-1}$ neutron-hole state at 5.230 MeV in ^{57}Ni, which is strongly excited via the ^{58}Ni(p, d)^{57}Ni reaction. The wave functions of the T=1 and T=2 GT states with the $f_{7/2}^{-1}$ neutron-hole configuration are inferred to be strongly coupled to 2p-2h configurations, making fragmented GT strengths in ^{58}Cu.

DOI: 10.1103/PhysRevC.68.064612 PACS number(s): 24.30.Cz, 25.55.Kr, 27.40.+z, 29.30.Ep

I. INTRODUCTION

Reaction processes mediated by the weak interaction often play decisive roles for testing nuclear models and for serving as input to understand astrophysical reaction chains. Some typical examples are (1) electron-capture processes leading to the presupernova phase before explosion, and (2) neutrino-nucleus reactions in type-II supernovae opening the way to synthesis of nuclear elements heavier than $A \geqslant 60$. The most important quantities in the processes mentioned above are the Gamow-Teller (GT) transitions in pf-shell nuclei with $A \sim 56$, which are the seeds of supernova explosions. Although a reasonable amount of data has been accumulated by studying the GT distributions in pf-shell nuclei, important data to check the validity of the model calculations and the effective interaction used are still not satisfactory to refine our knowledge of the nuclear-level structures.

The structures of the excited levels in nuclei heavier than the doubly magic nucleus ^{56}Ni provide good cases to test the validity of the model calculations and to extend their applicability to nuclei far from the β-stability line. The GT transitions from the ground state of ^{58}Ni to the excited states in ^{58}Cu are excellent candidates for the study of various coupling modes of collective one–particle-one-hole (1p-1h) excitations with two-particle–two-hole (2p-2h) configurations.

In ^{58}Cu, the proton-separation energy is relatively low (S_p=2.873 MeV). However, the one-neutron and two-proton separation energies are very high as S_n=12.426 MeV and S_{2p}=10.202 MeV, respectively. Because of the high S_n value, the states below E_x=12 MeV decay mainly by proton emission, and their widths are narrow (a few keV) due to the Coulomb barrier for proton emission. In fact, fragmented GT states have been observed in the high-resolution ^{58}Ni(^{3}He, t)^{58}Cu measurements at 450 MeV [1,2]. A single broad resonance at $E_x \sim 10$ MeV, which has been originally observed in the ^{58}Ni(p, n)^{58}Cu charge-exchange reactions [3–5], is now found to have a fine structure consisting of many fragmented GT states. This kind of fragmentation is caused by the coupling between 1p-1h and 2p-2h states via the residual interaction [6]. In the target nucleus ^{58}Ni with isospin T_0=1, fragmented $M1$ states with isospin quantum numbers of T=1 and T=2 are reported in (e, e'), (γ, γ'), and (p, p') measurements [7–14]. Therefore, the isobaric analogs (GT states) in ^{58}Cu corresponding to these $M1$ states in ^{58}Ni should be excited in charge-exchange reactions.

To clarify the isospin character and to understand the microscopic structure, it is of interest to measure decay by proton emission from the GT states in ^{58}Cu. Proton-decay strengths depend sensitively on the configurations of the wave functions. A charge-exchange process on ^{58}Ni mediated by the operator $\vec{\sigma}\cdot\vec{\tau}$ leads to a state with a neutron-hole and a proton-particle (1p-1h) configuration. This populates T=0, T=1, and T=2 states in ^{58}Cu with a ratio in excitation

strength determined by the isospin Clebsch-Gordan coefficients for T_0=1; $(2T_0-1)/(2T_0+1):1/(T_0+1):1/[(2T_0+1)(T_0+1)]$=2:3:1, respectively.

Proton emission leads to neutron-hole states with T=1/2 and T=3/2 in ^{57}Ni. The hole-state analogs (T=3/2) in ^{57}Ni have already been systematically studied via the ^{58}Ni$(p,d)^{57}$Ni reaction at 65 MeV [15,16]. Many fragmented $7/2^-$ and $3/2^-$ hole-state analogs have been reported above E_x=5.135 MeV in ^{57}Ni. Due to the isospin selection rule, proton emission from the T=2 GT states in ^{58}Cu into the T=1/2 states in ^{57}Ni is forbidden since decay by one nucleon only carries ΔT=1/2. Transitions from the T=1 states to both T=1/2 and T=3/2 states in ^{57}Ni are allowed. If one observes a strong feeding of proton decay from the excited GT states in ^{58}Cu into the T=3/2 states in ^{57}Ni, this provides good evidence that these states have T=2 character.

However, the final-state resolution of the ^{58}Ni(^{3}He, $t+p$)^{57}Ni experiment at 450 MeV is not good enough to resolve the fine structure of the isobaric-analog final states in ^{57}Ni, since the final-state resolution is dominated by the resolution of the used ^{3}He^{2+} beam. This prevents us from obtaining less unambiguous information on the structure of the GT resonance in ^{58}Cu. Thus, an additional complementary experiment was necessitated. To establish the final states in ^{57}Ni fed by proton emission from ^{58}Cu, we have obtained the ^{58}Ni(^{3}He, $t+\gamma$) coincidence data, which allows us to assign the final states in ^{57}Ni; thanks to a high-resolution γ-ray measurement with high-purity–Ge (HP-Ge) detectors. In the present paper, we report the results obtained from the ^{58}Ni(^{3}He, $t+p$) and ^{58}Ni(^{3}He, $t+\gamma$) coincidence experiments at 450 MeV to discuss the nature of the GT states in ^{58}Cu.

II. EXPERIMENT

A. Singles measurement

The experiments were carried out at the ring cyclotron facility of the Research Center for Nuclear Physics (RCNP), Osaka University. A ^{3}He^{2+} beam from the K=400 MeV ring cyclotron was used. The ^{3}He^{2+} beam was achromatically transported from the ring cyclotron to the target without any defining slits, and stopped in a Faraday cup inside the first dipole magnet $D1$ of the spectrometer Grand Raiden [17] which was set at 0°. The solid angle of the spectrometer was defined by a slit at the entrance of the spectrometer. The opening angles were ±30 mrad in the vertical direction, and ±20 mrad in the horizontal direction.

The target used was self-supporting ^{58}Ni foil with a thickness of 4.0 mg/cm^2 (99.9% enrichment). The ^{3}He^{2+} beam with an intensity of 2 nA was transported to the target under a low-background condition from beam halo. Tritons from the target were momentum analyzed in the spectrometer, and detected by multiwire drift chambers (MWDCs) at the focal plane. Ray-tracing technique allows us to obtain information on both the positions and the incidence angles of tritons at the focal plane of the spectrometer. The MWDCs were backed by three ΔE plastic scintillators with thicknesses of 1 mm, 10 mm, and 10 mm, respectively, for particle identification as well as for generating trigger signals for the coincidence measurements.

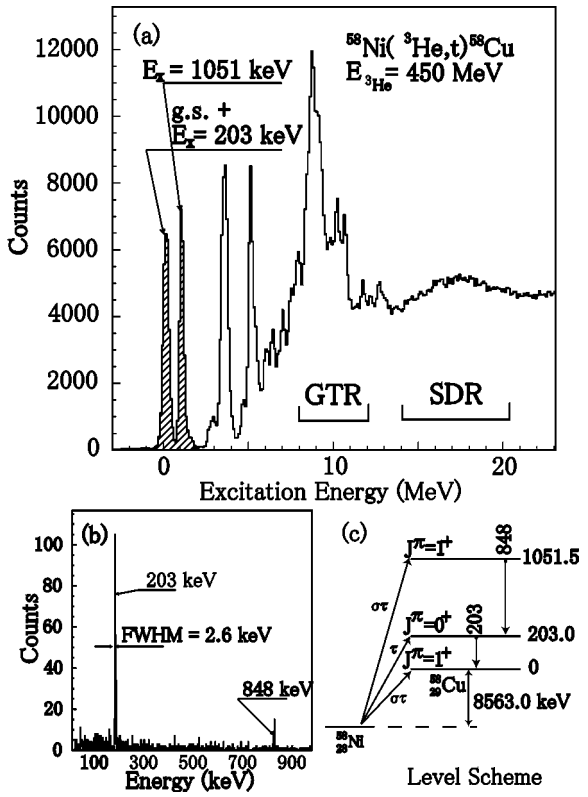

FIG. 1. (a) Singles spectrum of the ^{58}Ni(^{3}He, t)^{58}Cu reaction measured at 0° and a bombarding energy of 450 MeV. (b) Coincidence γ-ray spectrum of a Ge detector obtained by gating on the (^{3}He, t) peaks for the ground, 203-keV, and 1051-keV states. Two sharp γ-ray peaks at 203 keV and 848 keV are clearly visible. These γ rays are due to the decays from the 1051.5-keV (1^+) and 203.0-keV (0^+) states in ^{58}Cu. (c) Relevant levels in ^{58}Cu. Excitation modes via the (^{3}He, t) charge-exchange reaction and γ-ray decay scheme are indicated.

Figure 1(a) shows a typical spectrum of the ^{58}Ni(^{3}He, t)^{58}Cu reaction. Several discrete states in ^{58}Cu up to about 8 MeV have been reported to be 1^+ GT states in the high resolution (^{3}He, t) measurement using the dispersion-matching technique [2]. The bump at E_x=8–12 MeV is the Gamow-Teller resonance (GTR). The differential cross section for the GTR is strongly peaked at 0°, which is characteristic of ΔL=0 transitions. The global shape of the present (^{3}He, t) spectrum is similar to that obtained in the ^{58}Ni($p+n$)^{58}Cu reaction at 160 MeV and 0° by Rapaport *et al.* [4,5], who reported that the bump observed at E_x=8–12 MeV mostly consists of 1^+ states although a small amount of $J^\pi=2^+, 3^+$ components exists. The bump around E_x=18 MeV is the spin-dipole resonance (SDR). The differential cross section for the SDR is peaked around 1°, which is characteristic of ΔL=1 transitions at this bombarding energy.

To perform the present proton- and γ-coincidence measurements, reduction of beam halo was essential to obtain a good signal-to-noise ratio. Therefore, the achromatic transport technique of the ^{3}He beam was chosen. The energy resolution of the (^{3}He, t) experiment was 250 keV full width at half maximum (FWHM). The 1^+ ground state and the 0^+ isobaric analog state at E_x=203 keV were not resolved. Fig-

ure 1(b) demonstrates the usefulness of the coincidence measurement with γ-ray decay to identify the relevant excited states [shown in Fig. 1(c)].

B. Coincidence measurement for proton decay

Decay protons from the excited states in ^{58}Cu were detected in coincidence with tritons from the (^{3}He, t) reaction using an array system consisting of 37 lithium-drifted-silicon solid-state detectors (SSDs). Detection scheme of decay protons with the SSD detector has been described in detail in Ref. [18] although the number of SSDs is only 8. The SSDs are arranged at backward angles from 100° to 160° with respect to the ^{3}He beam in steps of 10°. The thickness of SSD is 5 mm with an area of 450 mm^2. The distance between the target center and each SSD is 150 mm. The solid angle covered by the SSD array is 5.7% of 4π geometry.

The energy resolution of SSDs was checked using a ^{241}Am α source ($E_{\alpha 1}$=5.487 MeV, 85.2%; $E_{\alpha 2}$ =5.443 MeV, 12.8%). The resolution was improved from 70 keV to 35 keV by cooling the detectors to a temperature of −25°C. However, the energy resolution for the final states in the ^{58}Ni(^{3}He, $t+p$) coincidence experiment was 300 keV in FWHM, mainly due to the limited resolution of the (^{3}He, t) spectra.

Since GT states are excited with $\Delta L=0$ angular momentum transfer, the correlation pattern of emitted protons is isotropic. The continuum background is due to the processes with three-body final states, such as the breakup-pickup reaction and the knock-on charge exchange. Therefore, the continuum background is strongly suppressed, by requiring coincidences between tritons at $\theta\sim 0°$ and decay protons at backward angles.

C. Coincidence measurement for γ decay

Decay γ rays were detected in coincidence with the (^{3}He, t) reaction. A special scattering chamber was prepared by using acrylic pipes with a thickness of 4 mm to measure low-energy γ rays without any serious reduction of detection efficiency. In the case of an acrylic plate with a thickness of 4 mm, for example, only 5.6% of the 203-keV γ rays are absorbed.

Four HP-Ge detectors are mounted at backward angles at a distance of ~150 mm from the target center to the detectors. The HP-Ge detector with a 60% volume is set at 125°, and the other three HP-Ge detectors with a 35% volume are placed at 97°, 125°, and 153°, respectively. The relative efficiencies of the HP-Ge detectors used were 60%, 35%, 35%, and 35% compared with the standard 3 in.×3 in. (7.62 cm ×7.62 cm) cylindrical NaI scintillation crystal. The energy dependence of the absolute efficiency for each γ-ray detector was determined using various γ-ray sources including a calibrated ^{152}Eu source.

A typical spectrum of γ rays emitted from the excited states in ^{58}Cu is shown in Fig. 1(b). The energy resolution of HP-Ge detectors was typically 2.6 keV for 203-keV γ rays. The counting rate of the γ-ray detectors was kept to be 70 kcps at maximum by controlling the ^{3}He beam current on the target. To check the gain shift of each detector, the background γ rays (834.8 keV from ^{54}Mn and 511.0 keV from positron annihilation) were monitored throughout the experimental runs. The gain shift was 1% at maximum during the entire experimental period, and was corrected for in the off-line analysis to generate the final γ-ray spectra by summing up all the good events from each detector.

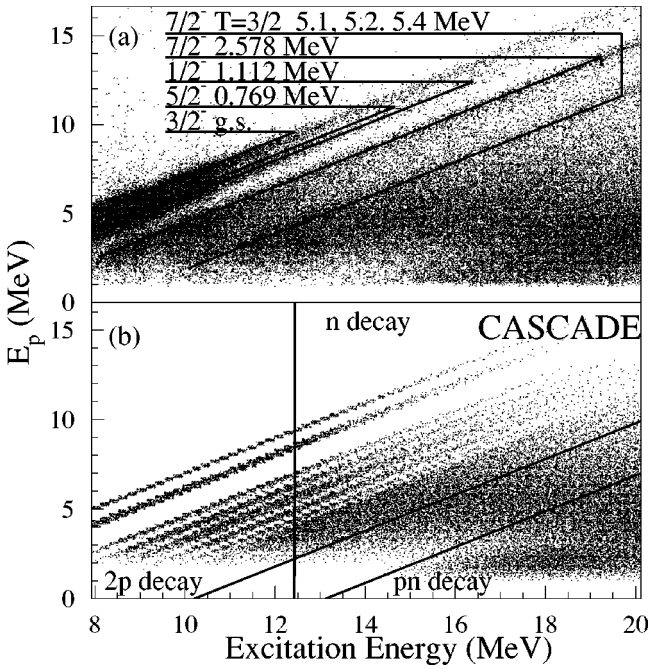

FIG. 2. (a) Two-dimensional scatter plot of proton-triton coincidence events induced by the ^{58}Ni(^{3}He, t) reaction at 0°. The loci indicate proton-decay events from the excited states in ^{58}Cu to the final states in ^{57}Ni. (b) Results of the statistical-model calculation with CASCADE [19].

III. RESULTS AND DISCUSSION

A. Proton decay

Figure 2(a) shows a two-dimensional scatter plot of proton energy versus E_x(^{58}Cu) for t-p coincidence events induced by the ^{58}Ni(^{3}He, t) reaction at 0°. The loci for proton decay from the excited states in ^{58}Cu to the 3/2$^-$ ground state, 5/2$^-$ at 0.769 MeV, 1/2$^-$ at 1.112 MeV, 7/2$^-$, T=1/2 at 2.578 MeV, and 7/2$^-$, T=3/2 at 5.1-, 5.2-, and 5.4-MeV states in ^{57}Ni can be identified as lines corresponding to $E_t+E_p\simeq$const. Figure 2(b) shows the results of a statistical-model calculation performed for decay protons from the excited states in ^{58}Cu, using the Hauser-Feshbach formalism with the code CASCADE [19].

In the calculation, spin, isospin, and parity of the reported excited states in ^{58}Cu, ^{57}Ni, ^{57}Cu, ^{56}Fe, and ^{56}Ni are used as the input parameters. Individual level parameters were taken from the experimental data compiled in Nuclear Data Sheets [20,22,21]. Global parameters for the level-density formula were used to describe the unknown levels at high excitation energies [23–25]. We took a procedure in making the level-density inputs in the CASCADE calculations similar to those given in Ref. [26]. Formation cross sections of ^{58}Cu were normalized to the ^{58}Ni(^{3}He, t) singles spectrum measured in

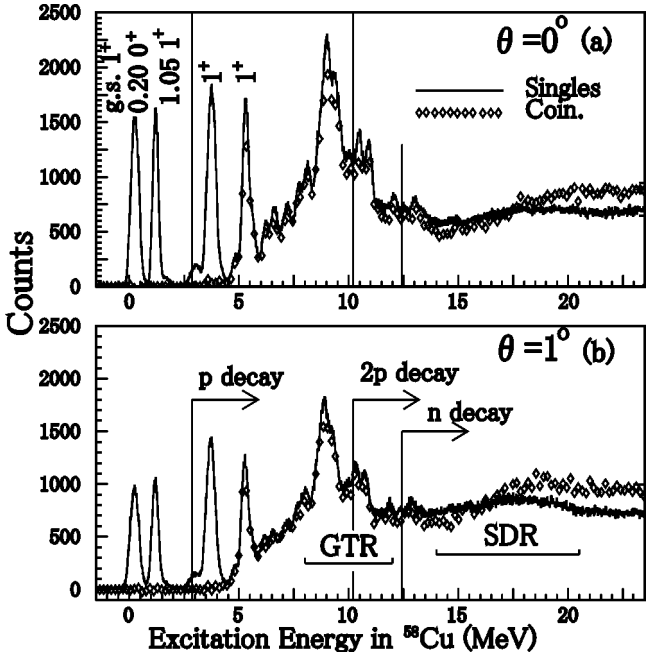

FIG. 3. Excitation-energy spectra for the ^{58}Ni(^{3}He, t) reaction at $E(^3\mathrm{He})=450$ MeV. The histograms represent the (^{3}He, t) singles spectra for scattering angles centered at $\theta=0°$ (a) and $\theta=1°$ (b). The diamonds ($\diamond$) represent the excitation-energy spectra gated on protons measured in coincidence by the SSDs. The particle-decay thresholds for proton decay ($S_p=2.873$ MeV), two-proton decay ($S_{2p}=10.202$ MeV), and neutron decay ($S_n=12.426$ MeV) are indicated as the vertical lines.

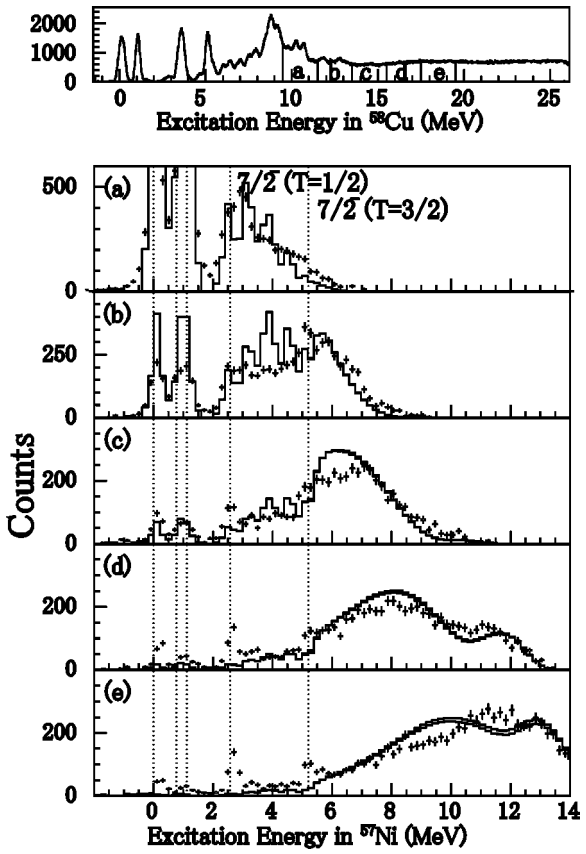

FIG. 4. Final-state spectra of the excited states in ^{57}Ni populated by proton decay from the excited states in ^{58}Cu. The spectra are obtained by projecting loci of Fig. 2(a) onto the ^{57}Ni excitation-energy axis. A singles ^{58}Ni(^{3}He, t) spectrum is shown in the upper part to indicate the gate positions (from 9.5 MeV to 19.5 MeV, in steps of 2 MeV) for each final-state spectrum denoted by (a)–(e). The dotted lines show the excitation energies for discrete levels in ^{57}Ni ($3/2^-$g.s., $5/2^-$ at 0.769 MeV, $1/2^-$ at 1.112 MeV, $7/2^-$, $T=1/2$ at 2.578 MeV, and $7/2^-$, $T=3/2$ at 5.1, 5.2, and 5.4 MeV). The experimental data are shown by the cross symbols. The results of the statistical-model calculation for proton decays from the $T=1$ and $T=0$ states in ^{58}Cu are shown by the solid histograms.

this experiment. The gross features of the proton-decay pattern agree with the results obtained in the statistical-model calculation. However, decay from the states at high excitation energies in ^{58}Cu to the low-lying discrete states in ^{57}Ni is enhanced in comparison with the results obtained in the statistical-model calculation. For example, the event locus corresponding to proton decay to the $7/2^-$, 2.578-MeV level in ^{57}Ni continuously extends to $E_x(^{58}\mathrm{Cu})=20$ MeV. This suggests that the SDR in ^{58}Cu has a wave function with the main $(\pi g_{9/2}\nu f_{7/2}^{-1})$ configuration and emits a proton from the $g_{9/2}$ orbit by the direct process to the $T=1/2$, $f_{7/2}^{-1}$ neutron-hole state in ^{57}Ni.

In Fig. 3, the singles spectra at $\theta=0°$ and $\theta=1°$ for the (^{3}He, t) reaction are compared with the (^{3}He, t) spectra gated on decay protons. For the states in the excitation-energy region from $S_p=2.873$ MeV to $S_n=12.426$ MeV, the branching ratio for proton decay is consistent with 100% except for the branching ratio for the 1^+ states just above the proton-decay threshold energy. Detection of the proton-decay events from the $E_x\sim3.5$ MeV peak was practically impossible due to the electronic noise threshold. The peak at $E_x\sim3.5$ MeV is due to the three states at $E_x=3.46$, 3.54, and 3.68 MeV which are reported in the work by Fujita *et al.* [2]. They were not resolved in the present (^{3}He, $t+p$) coincidence experiment.

The measured proton-decay branching ratio appears to exceed 100% above the two-proton-decay threshold ($S_{2p}=10.202$ MeV) if the increased multiplicity due to two proton emission is not taken into account. Since the available decay energies for each of the two protons are very low, the probability of emitting protons is strongly suppressed near the $2p$-decay threshold. Thus, the decay by one-proton emission dominates up to the neutron-decay threshold ($S_n=12.426$ MeV). When the neutron-decay channel opens, the proton-decay probability suddenly drops as observed at $E_x(^{58}\mathrm{Cu})=13-16$ MeV in the coincidence spectra shown in Fig. 3. However, the coincidence probability for decay protons increases from $E_x(^{58}\mathrm{Cu})\sim16$ MeV. This indicates that $2p$-decay events with a multiplicity of 2 increase with increasing the available emission energy. The present results from the (^{3}He, $t+\gamma$) coincidence measurement also support these conjectures.

In Fig. 4, the final-state spectra for the excited states in ^{57}Ni generated by gating on decay protons from excited states in ^{58}Cu are compared with the results of the statistical-model calculation. The calculated relative strengths of decay protons from the $T=0$ states and $T=1$ states in ^{58}Cu reproduce well the final-state spectra, irrespective of their excita-

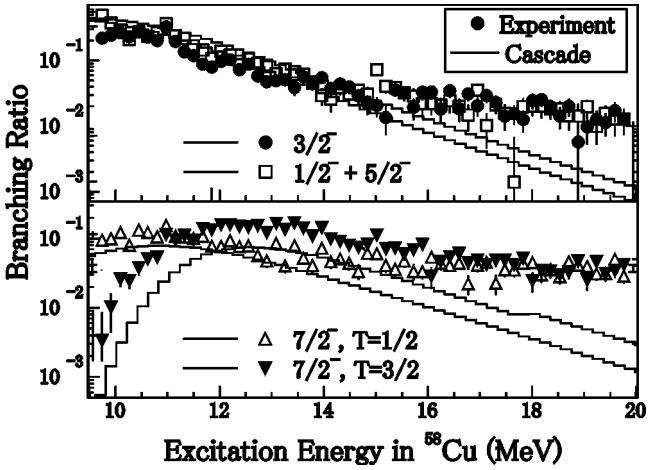

FIG. 5. Proton-decay branching ratios to the excited states in ^{57}Ni plotted as a function of the excitation energy in ^{58}Cu. The experimental branching ratios are shown for the $3/2^-$ (dots), $1/2^- + 5/2^-$ (open squares), $7/2^-, T=1/2$ (open triangles), and $7/2^-, T=3/2$ (solid triangles) states in ^{57}Ni. The lines represent the results of the statistical-model calculation.

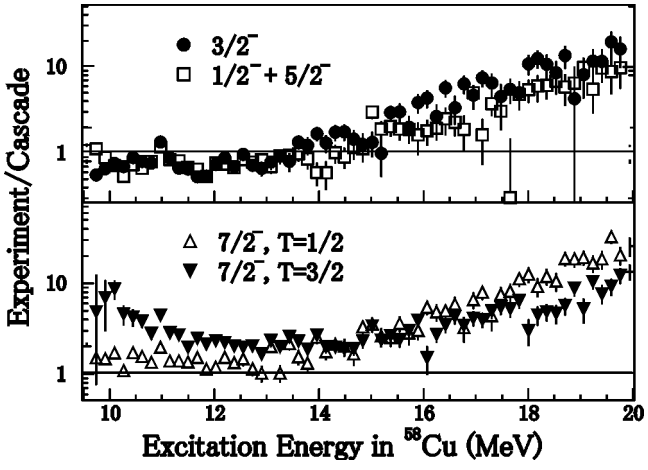

FIG. 6. Ratio between the experimental proton-decay branching ratio and the statistical-model calculations for the $3/2^-$ (dots), $1/2^- + 5/2^-$ (open squares), $7/2^-, T=1/2$ (open triangles), and $7/2^-, T=3/2$ (solid triangles) states in ^{57}Ni, respectively.

tion energies. Since most of the decay properties are characterized by the $T=1/2$ states in ^{57}Ni to which decay from $T=0$ states and $T=1$ states in ^{58}Cu is allowed, there is no significant difference between the decay patterns calculated for these $T=0$ and $T=1$ states as typically shown in Figs. 4(c), 4(d), and 4(e).

However, the proton-decay branching ratio for $T=2$ states in ^{58}Cu should be much different from other isospin states, because proton decay from $T=2$ states to $T=1/2$ states in ^{57}Ni is isospin forbidden. A statistical-model calculation code, which allows for three different isospin components in one nucleus, is not available at present. The modified and extended CASCADE code [19] allows for two isospin components starting from the ground-state isospin, e.g. in ^{58}Cu, $T=0$ and $T=1$. Therefore, it is not possible to treat proton decay from the $T=2$ states in ^{58}Cu to the $T=3/2$ states in ^{57}Ni. It is clear though that in a one-step process, without isospin mixing, $T=2$ states can only populate $T=3/2$ states by proton decay. Thus, we could not compare the experimental results with the statistical-model calculation for the proton decay from the $T=2$ states.

As seen in Figs. 4(c), 4(d), and 4(e), proton decays from the states at high excitation energies in ^{58}Cu into the $T=1/2, 7/2^-$ state at 2.578 MeV in ^{57}Ni are clearly observed. These proton decays are not predicted in the statistical-model calculation. In addition, proton decays into the $T=3/2, f_{7/2}^{-1}$ state at $E_x \sim 5.2$ MeV in ^{57}Ni have been identified in Figs. 4(d) and 4(e). This experimental observation indicates that the SDR with the wave function having mainly the $(\pi g_{9/2} \nu f_{7/2}^{-1})$ configuration directly decays to the $T=1/2, f_{7/2}^{-1}$ state in ^{57}Ni. However, from the present measurement, we cannot determine whether the SDR decays to the $T=3/2, f_{7/2}^{-1}$ state in ^{57}Ni, or the $T=2$, GT states coexisting with the SDR in ^{58}Cu decay to the $T=3/2$ states.

Figure 5 shows the proton-decay branching ratios to low-lying discrete states at $E_x=0.0$, 0.769, 1.112, 2.578, and ~ 5.2 MeV in ^{57}Ni. In the region above $E_x \sim 15$ MeV, the statistical-model calculations underestimate the proton-decay branching ratios. At $E_x \sim 19.5$ MeV, the discrepancy amounts to a factor of about 10. The direct-decay process, which is not included in the statistical-model calculations, is dominant in this energy region. In the lower excitation-energy region below $E_x \sim 15$ MeV, the statistical-model calculations seem to well reproduce the branching ratios for the $3/2^-$, $1/2^- + 5/2^-$, and $7/2^-$ ($T=1/2$) states. Proton decay from states at an excitation energy around 10 MeV to highly excited states in ^{57}Ni, such as the $7/2^-$ ($T=3/2$) state, is strongly suppressed due to the Coulomb barrier. Even under such conditions, the branching ratio for the $7/2^-$ ($T=3/2$) state is still high compared with the results of the statistical-model calculation (see the lower panel in Fig. 5). It is noteworthy to mention here that the statistical-model calculation underestimates the branching ratio to the $7/2^-$ ($T=3/2$) state for the entire excitation region by a factor of ~ 2–10. To show more clearly these discrepancies, we plotted the ratio between the experimental branching ratio and the statistical-model calculations (see Fig. 6). At $E_x=9.5$–11.5 MeV, the branching ratio to the $7/2^-$ ($T=3/2$) state in ^{57}Ni is enhanced by a factor of about 3 on average. This enhancement cannot be reproduced by the statistical-model calculation, which only takes into consideration the isospin states with $T=T_0=1$ and $T=T_0-1=0$. This is due to the fact that a sizable amount of the $T=2$ component exists at the bump region for the Gamow-Teller resonance above $E_x=9.7$ MeV, from where the $T=2$ states are expected to appear in ^{58}Cu [4].

B. γ Decay

Figure 7 shows a two-dimensional scatter plot of γ-triton coincidence events induced by the ^{58}Ni(^{3}He, t) reaction at 0°. The loci for γ decay indicate that several excited states in ^{58}Cu decay by proton emission into discrete final states in ^{57}Ni and ^{56}Co. The loci corresponding to the photopeaks due to these decay events are seen as horizontal lines in Fig. 7, i.e., in the case of γ decay subsequent to decay by nucleon

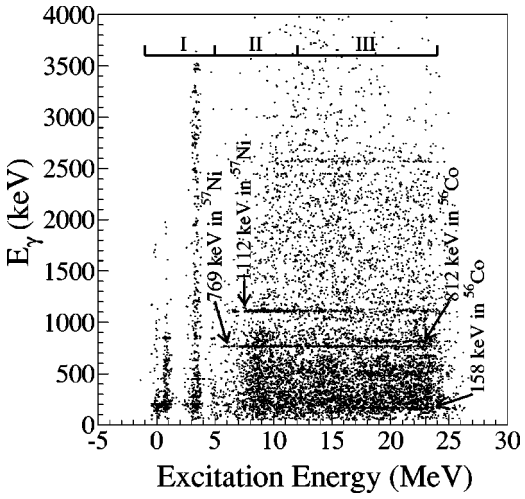

FIG. 7. Two-dimensional scatter plot of triton-γ coincidence events for the ^{58}Ni(^{3}He, t) reaction at 0°. Accidental events have been subtracted. The various loci indicate γ-decay events from the excited states of ^{58}Cu, ^{57}Ni, and ^{56}Co. For the clarification of the regions denoted as I (E_x=0–5 MeV), II (E_x=5–14 MeV), and III (E_x=14–24 MeV), see text.

emission from the giant-resonance region at E_x=8–24 MeV in ^{58}Cu. On the contrary, the loci corresponding to the γ-decay events from the discrete states between 0 and 5 MeV in ^{58}Cu are recognized. Event points dispersed in Fig. 7 are due to Compton-scattered events of coincident γ rays and due to events with a small photopeak. To understand the global features of the triton-γ coincidence data in more detail, decay patterns are examined by dividing the excitation energy in ^{58}Cu into three regions, I, II, and III.

In region I, γ-ray transitions from the discrete states in ^{58}Cu have been observed although the proton-decay threshold (S_p=2.873 MeV) opens. The photopeaks at 203, 444, and 3475 keV are clearly identified, suggesting that proton decay from the low-lying states in ^{58}Cu is largely suppressed due to the Coulomb barrier, and γ-decay competes with proton decay for the states at E_x<5 MeV.

The peaks corresponding to the states at E_x=3.460, 3.540, and 3.678 MeV were not resolved because we used an achromatic ^{3}He beam. To understand the decay schemes from these states, we examined the γ-ray transitions by gating the coincidence events on two halves of the unresolved peak at $E_x\sim$3.5 MeV. Figures 8(a) and 8(b) show the coincidence γ-ray spectra obtained by gating on the events in the divided peak regions E_x=3.17–3.62 MeV and E_x=3.62–4.20 MeV in the ^{58}Ni(^{3}He, t)^{58}Cu spectrum at 0°, respectively. It has been reported that the 3.460-MeV state is strongly excited in the energy region of E_x=3.17–3.62 MeV, and the 3.678-MeV state is strongly excited in the energy region of E_x=3.62–4.20 MeV via the (^{3}He, t) reaction at 0° [2]. The transition to the ground state was neither observed from the 3.460-MeV(1^+) state nor from the 3.678-MeV(1^+) state. Photopeaks for the 203-keV (0^+_{IAS})$\rightarrow$($1^+_{g.s.}$), the 444-keV (3^+_1)$\rightarrow$($1^+_{g.s.}$), the 3275-keV (1^+, 3.460 MeV)$\rightarrow$(0^+_{IAS}), and the 3475-keV (1^+, 3.678 MeV)$\rightarrow$(0^+_{IAS}) transitions were observed. A peak for the 3.678-MeV (1^+)$\rightarrow$0.444 MeV(3^+_1) transition was not clearly identified in this experiment. The results are summarized in Fig. 8(c).

TABLE I. Partial γ-decay branching ratios for the two states at 3.460 MeV and 3.678 MeV in ^{58}Cu. The branching ratios are given in %.

E_x (MeV)	Decay to	$\Gamma_\gamma/(\Gamma_p+\Gamma_\gamma)$ (%)
3.460	0.203 (0^+_{IAS})	38±11
3.678	0.203 (0^+_{IAS})	54±16
	0.444 (3^+_1)	31±6

The individual transition strength for the two states at 3.460 MeV and 3.678 MeV was not deduced in the analysis of the present (^{3}He, t) singles spectrum. However, the relative transition strengths of the states at 3.460 MeV and 3.678 MeV are reported by Fujita *et al.* [2]. Therefore, the transition strengths for the states at 3.460 MeV and 3.678 MeV were estimated by using the summed yield for a peak at ~3.5 MeV observed in the ^{58}Ni(^{3}He, t)^{58}Cu spectrum. The partial γ-decay branching ratios of the 3.460-MeV and 3.678-MeV states are given in Table I. The proton-decay branching ratios of the 3.460-MeV and 3.678

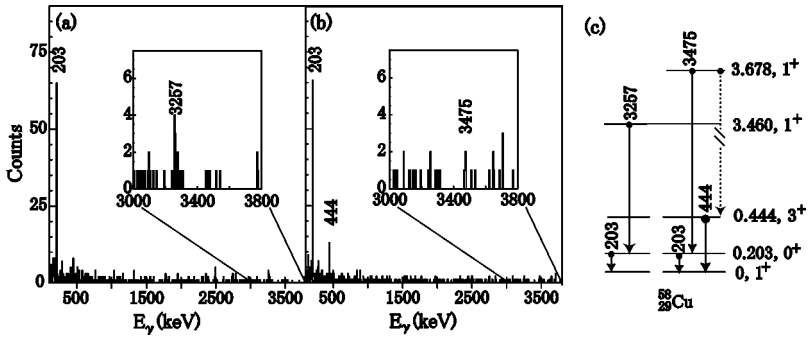

FIG. 8. (a) Coincidence γ-ray spectra obtained by gating on the events for the lower half peak at 3.17–3.62 MeV in the ^{58}Ni(^{3}He, t)^{58}Cu spectrum measured at 0°. Two γ rays at 203 and 3257 keV were observed. (b) Coincidence γ-ray spectra obtained by gating on the events for the upper half peak at 3.62–4.20 MeV. Three γ rays at 203, 444, and 3475 keV were observed. (c) Level scheme proposed for the low-lying states in ^{58}Cu. The labels for the γ decays are given in keV. The labels for the excited states in ^{58}Cu are given in MeV. The missing γ-ray transition is indicated by the dashed arrow.

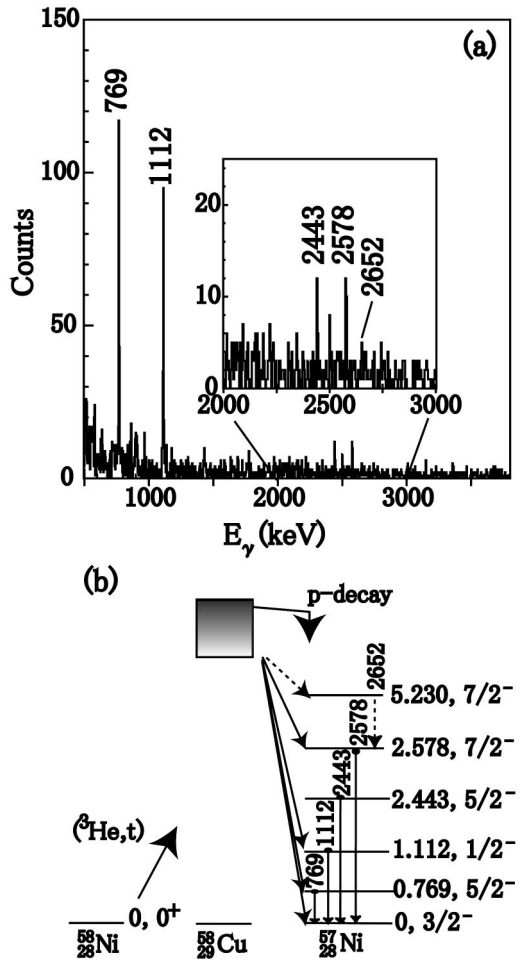

FIG. 9. (a) Coincidence γ-ray spectrum of a HP-Ge detector obtained by gating on the events for the GTR region at E_x =8–14 MeV in the ^{58}Ni(^{3}He, t)^{58}Cu spectrum at 0°. Photopeaks at 769, 1112, 2443, and 2578 keV correspond to the ground-state transitions from the excited states in ^{57}Ni. The dashed line inserted in the figure indicates the position of the γ-ray energy of 2652 keV, which is the transition energy from the 5.230-MeV state to the 2.578-MeV state. (b) Partial level scheme of ^{57}Ni. The labels for the γ decays are given in keV. The labels for the excited states in ^{57}Ni are given in MeV. Missing proton and γ transitions are indicated by the dashed arrows.

-MeV states, thus, amount to (62±11)% and (15±17)%, respectively.

In region II, γ-decay transitions cannot compete with proton decay anymore. The loci in this region mainly correspond to the events due to γ decays from the excited states in ^{57}Ni. Typically, two loci of the γ-decay events for the keV ($5/2^-_1 \rightarrow 3/2^-_{g.s.}$) and 1112 keV ($1/2^-_1 \rightarrow 3/2^-_{g.s.}$) transitions in ^{57}Ni are observed. The loci corresponding to these transitions continue to the high excitation energy of E_x ~24 MeV in ^{58}Cu. This indicates that the probability for direct proton decay is still not negligible for the states at high excitation energies in ^{58}Cu.

Comparing the results of the proton-decay measurement and the γ-decay measurement, it is possible to reveal the characteristics of the giant-resonance states in ^{58}Cu. Figure 9(a) shows the coincidence γ-ray spectrum obtained by gating on the events for the GTR region at E_x=8–14 MeV in the ^{58}Ni(^{3}He, t)^{58}Cu spectrum measured at 0°. Photopeaks at 796, 1112, 2443, and 2578 keV correspond to the ground-state transitions from the excited states in ^{57}Ni. The partial level scheme of ^{57}Ni is shown in Fig. 9(b). As mentioned in Sec. III A, the direct-decay protons from the GTR in ^{58}Cu to the $3/2^-$ ground state, $5/2^-$ at 0. MeV, $1/2^-$ at 1.112 MeV, $7/2^-$, T=1/2 at 2.578 MeV, and $7/2^-$, T=3/2 at 5.1-, 5.2-, and 5.4-MeV states in ^{57}Ni have been observed in the proton-decay measurement. In agreement with these facts, the 769-keV($5/2^-$)$\rightarrow$($3/2^-_{g.s.}$), 1112-keV($1/2^-$)$\rightarrow$($3/2^-_{g.s.}$), and 2578-keV($7/2^-$, T=1/2)$\rightarrow$($3/2^-_{g.s.}$) γ-decay transitions were clearly observed.

To corroborate the proton decay from the GTR in ^{58}Cu to the 2.578-MeV($7/2^-$, T=1/2) state in ^{57}Ni, the consistency of the 2578-keV γ-decay yields with the proton-decay data is examined. We observed 21±5 events for the 2578-keV peak in Fig. 9(a) in coincidence with the triton events for the GTR region at E_x=8–14 MeV in the ^{58}Ni(^{3}He, t)^{58}Cu spectrum at 0°. After the corrections of the absolute efficiencies, solid angles, and dead time, we obtained 28±4 for the γ-decay yields expected from the proton decay from the same 8–14 MeV GTR region to the 2.578-MeV state. This estimated number of 28±4 already exceeds the observed number of 21±5. Thus, the 2578-keV peak is considered to be mainly originated from the subsequent γ decay after the proton decay from the GTR in ^{58}Ni to the 2.578-MeV state in ^{57}Ni.

In the ^{58}Ni(p, d)^{57}Ni experiment by Ikegami *et al.* [15], the 5.230-MeV $7/2^-$ state is strongly excited in the T=3/2 region. On the base of the ^{58}Ni(^{3}He, $\alpha+\gamma$) experiment, Gould *et al.* reported that the 5.230-MeV, T=3/2 state decays strongly to the 2.578-MeV state with a branching ratio of 50% [27]. If we assume that 100% of the proton decay from the GTR in ^{58}Cu to the 5.2-MeV region in ^{57}Ni concentrates only to the state at E_x=5.230 MeV, 9.7±1.0 events for the 2652-keV γ peak are expected for the spectrum in Fig. 9(a). However, the measured counts are 7.0±4.6. It is very difficult to deduce any decisive conclusion from this statistical error. Reasonable conjecture deduced from the coincidence γ-decay yields for the 2578-keV and 2652-keV peaks is to attribute the observed facts to that the proton decay from the GTR in ^{58}Cu to the 5.230-MeV $7/2^-$ state in ^{57}Ni is very weak.

In region III, p-decay, n-decay, and pp-decay processes compete with each other. Several γ decays from excited states in ^{57}Ni and ^{56}Co are assigned. Two loci for the 970 keV (2^+_1)$\rightarrow$158 keV (3^+_1) and 158 keV (3^+_1) $\rightarrow$0 keV ($4^+_{g.s.}$) transitions in ^{56}Co have been observed. On the other hand, γ-ray decays from the excited states in ^{57}Cu have not been identified. One possible explanation for this experimental result is that there is no γ-ray transition in ^{57}Cu since the proton-decay threshold from ^{57}Cu to ^{56}Ni is extremely low (S_p=0.695 MeV).

When neutron decay occurs to excited levels in ^{57}Cu, the subsequent proton decay partially leads to excited levels in ^{56}Ni, from which γ decay is possible to be observed in the present experiment. However, we did not identify any 2701-keV γ-ray events from the transition 2701 keV (2^+_1)

$\rightarrow$0 keV ($0^+_{g.s.}$) in ^{56}Ni. Another plausible explanation is that there is no sizable neutron decay from the excited states in region III in ^{58}Cu since the (^{3}He, t) reaction at 450 MeV selectively excites the spin-flip T=2 GT states at high excitation energy from which neutron decay carrying only ΔT =1/2 is strongly suppressed in making the final T_0=−1/2 states in ^{57}Cu, and/or since the wave function of the SDR with the main ($\pi g_{9/2}\nu f^{-1}_{7/2}$) configuration does not allow such decay.

IV. SUMMARY

On the basis of the coincidence measurements of the (^{3}He, $t+p$) and (^{3}He, $t+\gamma$) reactions on ^{58}Ni, we have discussed the branching ratios for proton and γ decays from the GT states and the SDR in ^{58}Cu. The deduced branching ratios for proton decay from the T=0 and T=1 GT states are in good agreement with the results of the statistical-model calculation. The proton-decay strength from the GT states in ^{58}Cu to the 7/2$^-$, T=3/2 states in ^{57}Ni is not consistent with the results of the statistical-model calculation. The underestimation of the population of the 7/2$^-$, T=3/2 states in ^{57}Ni is qualitatively explained by the fact that the T=2 GTR component, which decays only to these states by isospin-allowed transitions, is not included explicitly in the statistical-model calculations. Therefore, a sizable amount of the T=2 GTR component, which the present statistical-model calculation code cannot deal with exactly, is inferred to exist in the bump region for the GT states above E_x=9.7 MeV.

In addition, we have confirmed that the T=1 and T=2 GT states do not strongly decay into a neutron-hole state at 5.230 MeV in ^{57}Ni, which is strongly excited via the ^{58}Ni(p, d)^{57}Ni reaction. The absence of proton decay into the 5.230-MeV 7/2$^-$ state is understood if the wave function of the GTR in ^{58}Cu does not have a dominant $1p-1h$ component and the proton-decay strengths do not strongly concentrate on any of three 7/2$^-$ states with isospin T=3/2 in ^{57}Ni [15]. These facts indicate that the wave functions of T=1 and T=2 GT states with the $f^{-1}_{7/2}$ neutron-hole configuration have a strong coupling to $2p-2h$ configuration, supporting the $2p$-$2h$ fragmentation mechanism for the GT resonances in nuclei [6].

The branching ratios for proton decay from the SDR in ^{58}Cu to the low-lying discrete states in ^{57}Ni are enhanced in comparison with the results of the statistical-model calculation. The SDR in ^{58}Cu is expected to have a wave function with the ($\pi g_{9/2}\nu f^{-1}_{7/2}$) configuration and strongly decays by the direct process to the T=1/2, $f^{-1}_{7/2}$ neutron-hole state in ^{57}Ni.

We did not observe any γ rays due to the deexcitations from the low-lying states in ^{57}Cu and in ^{56}Ni subsequent to neutron decays from the SDR in ^{58}Cu and/or proton decays from ^{57}Cu. This result is understood in terms of the isospin selection rule. In the case of T=2 states at high excitation energies in ^{58}Cu, neutron decay with an isospin transfer of ΔT=1/2 is forbidden to final T=1/2,T_z=−1/2 states in ^{57}Cu. However, the (^{3}He, t) reaction at 450 MeV excites both T =1 and T=2 states at high excitation energies. Thus, the SDR with T=1 coexists with the T=2 GTR there. Although the decay of T=1 states to final T=1/2,T_z=−1/2 states in ^{57}Cu is isospin allowed, the wave functions of the SDR with the main ($\pi g_{9/2}\nu f^{-1}_{7/2}$) configuration seems to suppress such decay.

The present results will serve to establish a good understanding of the fragmented fine structure of the GTR in ^{58}Cu. Further theoretical work including the development of the statistical-model calculation with T=2 is required to describe the fine structure of the GTR as well as the decay properties of the GTR and SDR in ^{58}Cu.

ACKNOWLEDGMENTS

The authors would like to thank the RCNP cyclotron staff for providing a clean and stable ^{3}He beam to complete this difficult experiment. We are grateful to Dr. M. Ohshima and Dr. T. Murakami for allowing us to use their HP-Ge detectors in the present experiment. This work was supported in part by the Ministry of Education, Culture, Sports, Science and Technology of Japan, by the U.S. National Science Foundation (NSF), and by the Japan Society for the Promotion of Science (JSPS) under the US-Japan Cooperative Science Program.

[1] H. Akimune, I. Daito, Y. Fujita, M. Fujiwara, M. B. Greenfield, M. N. Harakeh, T. Inomata, J. Jänecke, K. Katori, S. Nakayama, H. Sakai, Y. Sakemi, M. Tanaka, and M. Yosoi, Nucl. Phys. **A569**, 245c (1994).

[2] Y. Fujita, H. Fujita, T. Adachi, G. P. A. Berg, E. Caurier, H. Fujimura, K. Hara, K. Hatanaka, Z. Janas, J. Kamiya, T. Kawabata, K. Langanke, G. Martínez-Pinedo, T. Noro, E. Roeckl, Y. Shimbara, T. Shinada, S. Y. van der Werf, M. Yoshifuku, M. Yosoi, and R. G. T. Zegers, Eur. Phys. J. A **13**, 411 (2002).

[3] C. Gaarde, J. S. Larsen, and J. Rapaport, in *Spin Excitations in Nuclei*, edited by F. Petrovich *et al.* (Plenum, New York, 1984), p. 65.

[4] J. Rapaport, T. Taddeucci, T. P. Welch, D. J. Horen, J. B. McGrory, C. Gaarde, J. Larson, E. Sugarbaker, P. Koncz, C. C. Foster, C. D. Goodman, C. A. Goulding, and T. Masterson, Phys. Lett. **119B**, 61 (1982).

[5] J. Rapaport, T. Taddeucci, T. P. Welch, C. Gaarde, J. Larson, D. J. Horen, E. Sugarbaker, P. Koncz, C. C. Foster, C. D. Goodman, C. A. Goulding, and T. Masterson, Nucl. Phys. **A410**, 371 (1983).

[6] A. Arima, K. Shimizu, W. Bentz, and H. Hyuga, Adv. Nucl. Phys. **18**, 1 (1987).

[7] R. A. Lindgren, W. L. Bendel, E. C. Jones., L. W. Fagg, X. K. Maruyama, J. W. Lightbody Jr., and S. P. Fivozinsky, Phys. Rev. C **14**, 1789 (1976).

[8] R. Frey, A. Friebel, H. D. Gräf, T. Grundey, G. Kühner, W. Mettner, D. Meuer, A. Richter, G. Schrieder, A. Schwierczin-

ski, E. Spamer, O. Titze, and W. Knüpfer, J. Phys. Soc. Jpn. **44**, 202 (1978).

[9] K. Ackermann, K. Bangert, U. E. P. Berg, G. Junghans, R. K. M. Schneider, R. Stock, and K. Wienhard, Nucl. Phys. **A372**, 1 (1981).

[10] N. Anantaraman, G. M. Crawley, A. Galonsky, C. Djalali, N. Marty, M. Morlet, A. Willis, and J.-C. Jourdain, Phys. Rev. Lett. **46**, 1318 (1981).

[11] G. M. Crawley, N. Anantaraman, A. Galonsky, C. Djalali, N. Marty, M. Morlet, A. Willis, J.-C. Jourdain, and P. Kitching, Phys. Rev. C **26**, 87 (1982).

[12] C. Djalali, N. Marty, M. Morlet, A. Willis, J.-C. Jourdain, N. Anantaraman, G. M. Crawley, and A. Galonsky, Nucl. Phys. **A388**, 1 (1982).

[13] M. Fujiwara, Y. Fujita, I. Katayama, S. Morinobu, T. Yamazaki, H. Ikegami, S. I. Hayakawa, and K. Katori, Nucl. Phys. **A410**, 137 (1983).

[14] W. Mettner, A. Richter, W. Stock, B. C. Metsch, and A. G. M. van Hees, Nucl. Phys. **A473**, 160 (1987).

[15] H. Ikegami, T. Yamazaki, S. Morinobu, I. Katayama, M. Fujiwara, Y. Fujita, H. Taketani, M. Adachi, T. Matsuzaki, N. Koori, and M. Matoba, Nucl. Phys. **A329**, 84 (1979).

[16] H. M. Sen Gupta, Syafarudin, S. Aoki, F. Aramaki, M. Matoba, Y. Uozumi, G. Wakabayashi, T. Sakae, N. Koori, T. Maki, M. Nakano, Y. Fujita, M. Fujiwara, H. Ikegami, I. Katayama, S. Morinobu, and T. Yamazaki, Phys. Rev. C **63**, 017601 (2000). Note that the excitation energies above $E_x \sim 4$ MeV presented in this work are systematically deviated from the compilation values (see Ref. [22]).

[17] M. Fujiwara, H. Akimune, I. Daito, H. Fujimura, Y. Fujita, K. Hatanaka, H. Ikegami, I. Katayama, K. Nagayama, N. Matsuoka, S. Morinobu, T. Noro, M. Yoshimura, H. Sakaguchi, Y. Sakemi, A. Tamii, and M. Yosoi, Nucl. Instrum. Methods Phys. Res. A **422**, 484 (1999).

[18] H. Akimune, I. Daito, Y. Fujita, M. Fujiwara, M. B. Greenfield, M. N. Harakeh, T. Inomata, J. Jänecke, K. Katori, S. Nakayama, H. Sakai, M. Tanaka, and M. Yosoi, Phys. Rev. C **52**, 604 (1995).

[19] F. Pühlhofer, Nucl. Phys. **A280**, 267 (1977); M. N. Harakeh, Computer code CASCADE, extended version.

[20] M. R. Bhat, Nucl. Data Sheets **80**, 789 (1997).

[21] H. Junde, Nucl. Data Sheets **67**, 523 (1992).

[22] M. R. Bhat, Nucl. Data Sheets **85**, 415 (1998).

[23] E. Gadioli and R. Zetta, Phys. Rev. **167**, 1016 (1968).

[24] W. Dilg, W. Schantl, H. Vonach, and M. Uhl, Nucl. Phys. **A217**, 269 (1973).

[25] W. D. Myers, *Droplet Models of Atomic Nuclei* (Plenum, New York, 1977).

[26] R. G. T. Zegers, S. Brandenburg, M. N. Harakeh, S. Y. van der Werf, J. Jänecke, T. O'Donnell, D. A. Roberts, S. Shaheen, G. P. A. Berg, C. C. Foster, T. Rinckel, and E. J. Stephenson, Phys. Rev. C **61**, 054602 (2000).

[27] C. R. Gould, D. P. Balamuth, P. F. Hinrichsen, and R. W. Zurmühle, Phys. Rev. **188**, 1792 (1969).